JOURNAL OF AGRICULTURAL AND FOOD CHEMISTRY

Article

pubs.acs.org/JAFC

Tetramethylammonium Hydroxide (TMAH) Thermochemolysis for Probing in Situ Softwood Lignin Modification in Each Gut Segment of the Termite

Jing Ke, Dhrubojyoti D. Laskar, and Shulin Chen*

Department of Biological Systems Engineering, Washington State University, Pullman, Washington 99164-6120, United States

ABSTRACT: Termites are highly effective in lignocellulose degradation; however, the process of lignin deconstruction along the alimentary canal is not well understood. In this study, the wood metabolites in each gut segment were tentatively analyzed using pyrolysis−gas chromatography−mass spectrometry in the presence of tetramethylammonium hydroxide. Collectively, the significant differences in the pyrolysate distribution among each sample established (1) conservation of the major β-O-4′ bonds of lignin during termite digestion, although a selective lignin substructure modification was observed across the whole gut; (2) initiation of lignin−polysaccharide dissociation, aliphatic oxidation/carboxylation, phenolic dehydroxylation in the foregut, and linkage modification of the 5-5′, β-5′, and β-1′ substructures; (3) the continuation of foregut reactions into the midgut with further phenolic carboxylation/demethoxylation/carbonylation; and (4) phenolic/aliphatic esterifications in the hindgut. Overall, elucidation of the stepwise lignin unlocking mechanism in termites provides a valuable insight for understanding plant cell wall structure and its recalcitrance.

KEYWORDS: *wood-feeding termite, softwood tissue, stepwise lignin unlocking, gut segment*

INTRODUCTION

The heterogeneous and irregular arrangement of lignin construction results in resistance to saccharification, which severely limits the enzymatic conversion of lignocellulosic biomass to fermentable sugars. When hydrolytic enzymes are applied to release plant sugars for biodiesel or bioethanol production, lignin aggregates bind to the enzymes and reduce the efficiency of the conversion.[1−3] Because cellulose can be fully digested only after dissociation of the lignin framework from the complex lignocellulosic matrix, it is important to understand the effective lignin disruption processes and to what extent lignin content and composition should be modified for efficient downstream cellulose saccharification.[4] Nature, through the evolutionary process, has developed biological systems, such as termites, that can efficiently extract energy from plant materials by effective deconstruction of lignocellulose under natural conditions. Biological systems are the proof-of-concept of what can be physically achieved;, and with adequate understanding, these biological systems can be harnessed or modeled for improved utilization of renewable lignocellulosic biomass.

The high efficiency of cellulose utilization by wood-feeding termites in terms of rate and extent (up to 95% cellulose conversion in wood within 24 h) makes it a promising biological model system for biomass utilization. By understanding and mimicking its unique pretreatment system, we can develop new technology to achieve higher efficiency. The digestion process of the termite begins from the mandibles, where woody biomass is masticated into small particle sizes. As the particles are moved along the digestive tract, which includes the foregut, midgut, and hindgut, various catalysts are utilized in sequence, and the substrates are treated under different physical, chemical, and biochemical conditions that function synergistically to effectively deconstruct the plant biopolymers. The termite foregut performs as a valve system (crop-filter chamber) and as the storage and initial digestion organ. The midgut is the main organ for secretion of digestive enzymes by the epithelial cells, and the hindgut has a microbial niche environment, which promotes synergistic cellulose hydrolysis. Accordingly, our obtained results indicate that termite-induced lignin pretreatment is not achieved by severe and direct degradation, but rather through selective modification of functional groups and cleavage of ether linkages within lignin and ester/ether linkages between lignin−hemicellulose and lignin−cellulose.[5−7] The modified lignin in this process allows enzymes used in saccharification to more easily access the cellulose and hemicellulose.[8,9]

Pyrolysis methods involving thermally assisted methylation with tetramethylammonium hydroxide (TMAH) have emerged as a powerful methodology for characterizing polymers.[10−14] Co-injection of TMAH during pyrolysis provides more flexibility to acquire structural information compared to conventional pyrolysis, because it protects thermolabile compounds and allows the chromatographic separation of both polar and nonpolar targets in the same run, which allows for the subsequent methylation of −COOH and −OH groups on lignin.[15−18] The combination of pyrolysis and in situ methylation using TMAH to depolymerize the fragments through methylation of methyl esters from carboxylic acids and methyl ethers from alcohols/phenols is a simple and efficient method for the characterization of lignin-derived compounds. Methylation of polar compounds formed from pyrolysis renders them more volatile and less polar so that they can be

Received: July 10, 2012
Revised: January 9, 2013
Accepted: January 20, 2013
Published: January 21, 2013

dx.doi.org/10.1021/jf3048548 | J. Agric. Food Chem. 2013, 61, 1299−1308

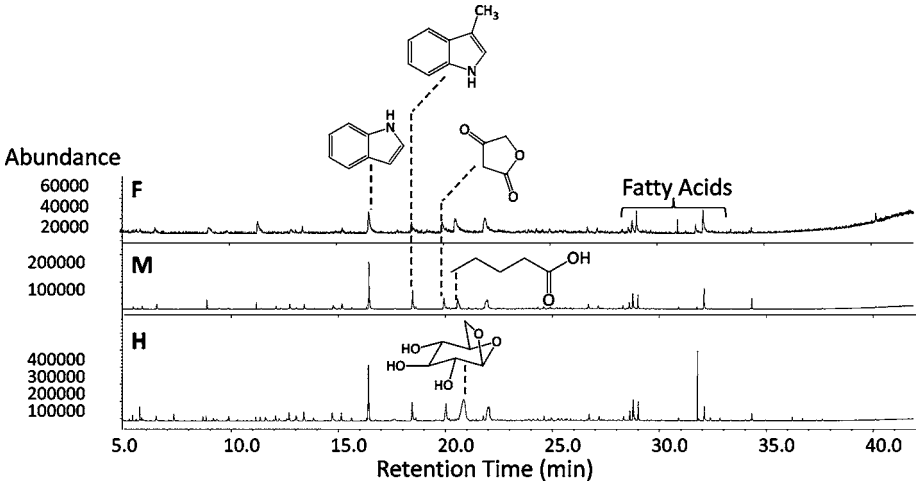

Figure 1. TIC of Py-GC-MS profiles of the foregut (F), midgut (M), and hindgut (H) from cellulose-fed termite in the presence of TMAH.

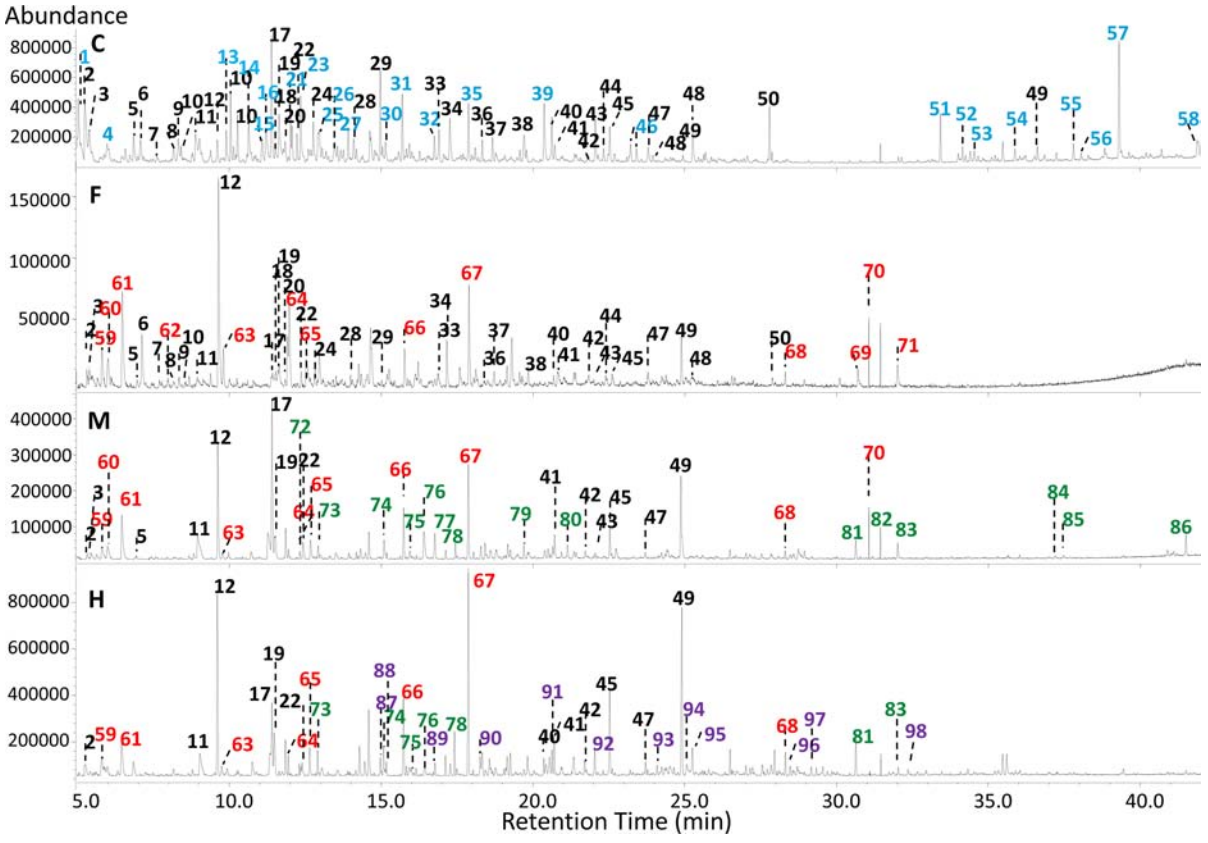

Figure 2. Flash pyrolysis with GC-MS profiles of undigested softwood control (C) and termite foregut (F), midgut (M), and hindgut (H) in the presence of TMAH. The peaks labeled 59−97 in the gut content chromatograms are new pyrolysates that appeared after termite digestion. All of the peaks indicated in the undigested control spectrum without labeling in the gut samples are pyrolysates that disappeared in termite gut. Peaks labeled in blue refer to structures showing in control and disappearing in foregut samples, the red ones are structures first showing in foregut and disappearing in midgut, the green ones to structures first showing in midgut but disappearing in hindgut, and the purple ones stand for structures newly appearing in hindgut. The structure assignments for the labeled peaks are shown in Figure 3.

analyzed more readily by GC, and pyrolytic intermediate reactions are subsequently minimized.[13] The pyrolysis−methylation process could avoid the loss of structural information of biomass. This method has proved to be a very useful technique for the characterization of polymers[19] and also the in situ analysis of lignin in biomass.[20] Likewise, we have successfully characterized termite feces by employing this method.[7]

The rationale of this study is based on the superior performance of the worker caste of wood-feeding termite *Coptotermes formosanus* (Shiraki) on cellulose utilization[21] and stepwise introduction of specific reactions on lignin,[5,22] as well as the varied microparameters for lignin structural modification in each gut section.[5] Actually, termite gut contents have been analyzed by conventional pyrolysis−gas chromatography−mass spectrometry (Py-GC-MS).[5] Although it is possible to obtain

dx.doi.org/10.1021/jf3048548 | J. Agric. Food Chem. 2013, 61, 1299−1308

Table 1. Tentative Identification of Pyrolysis Products of Softwood and Fore-, Mid-, and Hindgut Contents

			percentage[a]			
no.	RT (min)	compound	control	foregut	midgut	hindgut
1	5.0	2(3*H*)-furanone, dihydro-3-methyl-	1.55	×	×	×
2	5.2	2-cyclopenten-1-one	2.18	0.64	0.52	1.54
3	5.4	2-cyclopenten-1-acetaldehyde, 2-oxo-	0.68	0.21	0.78	×
4	6.0	1,3-cyclopentadiene, 5-(1-methylethylidene)-	0.25	×	×	×
5	6.8	2-cyclopenten-1-one, 2-methyl-	0.86	0.38	0.35	×
6	7.7	benzene, methoxy-	0.75	4.52	×	×
7	7.6	2-cyclopenten-1-one, 3,4-dimethyl-	0.13	0.12	×	×
8	8.2	benzaldehyde	0.47	0.86	×	×
9	8.3	2-cyclopenten-1-one, 3-methyl-	0.74	0.84	×	×
10	8.4	cyclopentene, 3,5-dimethoxy-	2.95	0.32	×	×
11	8.9	phenol	0.98	1.58	5.48	3.39
12	9.6	benzene, 1-methoxy-4-methyl-	0.65	18.91	11.18	13.03
13	9.9	2-cyclopenten-1-one, 2-hydroxy-3-methyl-	0.69	×	×	×
14	10.6	phenol, 2-methyl-	1.07	×	×	×
15	11.1	2,5-furandione, 3-(1,1-dimethylethyl)-	0.84	×	×	×
16	11.2	phenol, 3-methyl-	1.35	×	×	×
17	11.4	phenol, 2-methoxy-	3.04	1.27	14.69	3.72
18	11.5	benzoic acid, methyl ester	0.32	0.65	×	×
19	11.6	2-cyclopenten-1-one, 2-hydroxy-3-methyl-	1.58	2.18	2.33	3.20
20	11.8	phenol, 2,6-dimethyl-	0.38	0.49	×	×
21	12.1	furan, tetrahydro-2-(methoxymethyl)-	0.58	×	×	×
22	12.2	methoxyacetic acid, 2-tetrahydrofurylmethyl ester	0.61	1.06	1.95	1.04
23	12.4	2,3′-bifuran, 2,2′,3′,5-tetrahydro-	1.81	×	×	×
24	12.8	benzene, 1,2-dimethoxy-	0.99	1.71	×	×
25	13.0	phenol, 2,4-dimethyl-	1.56	×	×	×
26	13.5	phenol, 3,4-dimethyl-	0.65	×	×	×
27	13.9	phenol, 2-methoxy-4-methyl-	0.77	×	×	×
28	14.1	benzaldehyde, 3-methoxy-	0.55	0.70	×	×
29	15.0	2,3-dimethoxytoluene	2.05	0.27	×	×
30	15.1	benzenemethanol, 3-hydroxy-5-methoxy-	0.52	×	×	×
31	15.7	α-D-xylofuranoside, methyl 2,5-di-*O*-methyl-	1.81	×	×	×
32	16.8	2-methoxy-4-vinylphenol	0.60	×	×	×
33	16.9	benzene, 4-ethyl-1,2-dimethoxy-	0.81	1.52	×	×
34	17.3	phenol, 3,4-dimethoxy-	1.48	3.86	×	×
35	17.9	benzene, 4-ethenyl-1,2-dimethoxy-	1.50	×	×	×
36	18.4	2,3,6-tri-*O*-methyl-D-galactopyranose	0.47	0.45	×	×
37	18.7	benzene, 1,2-dimethoxy-4-(2-propenyl)-	0.60	1.26	×	×
38	19.7	phenol, 2-methoxy-5-(1-propenyl)-, (*E*)-	0.90	1.13	×	×
39	20.4	benzene, 1,2-dimethoxy-4-(1-propenyl)-	1.98	×	×	0.88
40	20.6	benzaldehyde, 3,4-dimethoxy-	1.09	0.65	×	×
41	20.7	1,4-benzenedicarboxylic acid, dimethyl ester	0.38	1.65	1.78	2.33
42	21.8	1-propanone, 1-(2,4-dimethoxyphenyl)-	0.17	0.93	0.53	0.79
43	22.1	ethanone, 1-(3,4-dimethoxyphenyl)-	1.22	0.32	0.44	×
44	22.3	3,4-dimethoxyphenylacetone	0.35	0.44	×	×
45	22.5	benzoic acid, 3,4-dimethoxy-, methyl ester	0.75	0.80	2.38	5.84
46	23.0	1,2-dimethoxy-4-(2-methoxyethenyl)benzene	0.77	×	×	×
47	23.8	propiophenone, 3′,4′-dimethoxy-	0.49	1.26	0.61	0.69
48	24.0	1,2-dimethoxy-4-(3-methoxy-1-propenyl)benzene	1.44	×	×	×
49	24.9	4-phenylbutyric acid, 4′,5′-dimethoxy-	0.16	3.33	8.83	12.63
50	27.8	1,2,3,4-tetramethylmannose	3.90	0.71	×	×
51	33.4	D-glucopyranoside, methyl 2,3,4-tri-*O*-methyl-	8.58	×	×	×
52	34.2	D-arabino-hexopyranoside, methyl 2,6-dideoxy-4-*O*-(6-deoxy-3-*O*-methyl-β-D-allopyranosyl)-3-*O*-methyl-	2.32	×	×	×
53	34.5	1,1′-biphenyl, 4,4′,5′,6′-tetramethoxy-	2.11	×	×	×
54	35.9	α-D-mannopyranoside, methyl 2,3,4,6-tetra-*O*-methyl-	2.13	×	×	×
55	37.8	fluoren-9-ol, 3,6-dimethoxy-9-(2-phenylethenyl)-	3.10	×	×	×
56	38.1	veratril	1.46	×	×	×
57	39.3	3,3′,4,4′-tetramethoxystilbene	21.77	×	×	×
58	41.9	carissanol dimethyl ether	6.09	×	×	×
59	5.8	ethylbenzene	×	3.31	1.86	1.66

dx.doi.org/10.1021/jf3048548 | *J. Agric. Food Chem.* 2013, 61, 1299−1308

Table 1. continued

no.	RT (min)	compound	percentage[a] control	foregut	midgut	hindgut
60	6.0	benzene, 1,3-dimethyl-	×	3.58	2.17	×
61	6.5	styrene	×	9.64	6.25	3.95
62	8.0	propylbenzene	×	0.61	×	×
63	9.8	1-(2-methylphenyl)ethanol	×	2.20	0.64	0.61
64	12.0	benzene, 1-ethyl-4-methoxy-	×	4.99	0.54	0.57
65	12.5	1,3-cyclopentanedione, 4,4-dimethyl-	×	3.58	2.02	2.09
66	15.8	1*H*-indole, 1-methyl-	×	2.85	4.46	5.36
67	17.9	1*H*-indole, 1,2-dimethyl-	×	8.07	8.52	13.76
68	28.3	[1,1′-biphenyl]-4,4′-dicarboxylic acid, dimethyl ester	×	0.69	0.55	1.33
69	30.7	benzene, 1,1′-(1,2-ethanediyl)bis[4-methoxy-	×	1.28	×	×
70	31.0	benzoic acid, 2-phenoxy-, methyl ester	×	1.88	0.90	×
71	32.0	4*H*-1-benzopyran-4-one, 7-(*β*-D-glucopyranosyloxy)-5-hydroxy-2-(4-methoxyphenyl)-	×	2.12		
72	12.3	isonicotinic acid *N*-oxide	×	×	0.57	×
73	12.9	benzene, 1-ethenyl-4-methoxy-	×	×	0.86	1.24
74	15.1	benzaldehyde, 3-(phenylmethoxy)-	×	×	1.90	1.76
75	16.0	ethanone, 1-(2,4-dihydroxyphenyl)-	×	×	0.76	0.33
76	16.4	indole	×	×	4.14	0.81
77	16.9	ethanone, 1-(2-hydroxy-5-methylphenyl)-	×	×	2.49	×
78	17.5	piperoxan	×	×	1.13	2.58
79	19.7	phenol, 2-methoxy-4-(1-propenyl)-	×	×	1.07	×
80	21.1	2,4′-dihydroxy-3′-methoxyacetophenone	×	×	1.14	×
81	30.7	benzene, (1-methoxy-4-methyl-3-pentenyl)-	×	×	1.61	2.50
82	31.4	methyl (methyl 2-*O*-methyl-*α*-D-mannopyranoside) uronate	×	×	0.95	×
83	32.0	benzofuran-3-one, 2-[3-hydroxy-4-methoxybenzylidene]-6-hydroxy-	×	×	1.19	0.54
84	37.2	1,2-dimethoxy-4-(1,2,3-trimethoxypropyl)benzene	×	×	0.29	×
85	37.5	6*H*-benzofuro[3,2-*c*][1]benzopyran, 3,9-dimethoxy-	×	×	0.29	×
86	41.5	1-hydroxy-2-(2,3,4,6-tetra-*O*-acetyl-*β*-D-glucopyranosyl)-9*H*-xanthene-3,6,7-triyl triacetate	×	×	1.86	×
87	15.0	benzoic acid, 3-methoxy-	×	×	×	0.68
88	15.2	emimycin	×	×	×	0.58
89	16.8	4-acetoxy-3-methoxystyrene	×	×	×	0.90
90	18.3	2-propenoic acid, 3-phenyl-, methyl ester	×	×	×	0.92
91	20.6	allyl *p*-(2-hydroxyethoxy)benzoate	×	×	×	1.57
92	22.1	1-propanone, 1-(2,4-dimethoxyphenyl)-	×	×	×	1.89
93	24.1	2-propenoic acid, 3-(4-methoxyphenyl)-, methyl ester	×	×	×	0.57
94	25.1	1-(2-vinylphenyl)propan-1-one	×	×	×	1.24
95	25.3	2-propenoic acid, 3-[4-(acetyloxy)-3-methoxyphenyl]-, methyl ester	×	×	×	1.74
96	28.5	benzoic acid, 4-(5-formyl-2-furanyl)-	×	×	×	0.68
97	29.2	3-phenylbutyrophenone	×	×	×	0.60
98	32.4	furan-2-carboxylic acid, 4-benzyloxyphenyl ester	×	×	×	0.48

[a]The percentages of pyrolysates in the total labeled pyrolysates. ×Not detected in the pyrogram.

accurate quantitative analysis of monomeric lignin composition by Py-GC-MS, this technique is somewhat restrained toward analysis (by GC-MS) of polar pyrolysates generated from nitrogenous material associated with the secondary reactions of pyrolysates during the pyrolytic process.[10] To provide more conclusive evidence and further insight into the associated role played by each gut segment at a structural level in the softwood lignin during the termite digestion process, the advanced analysis of TMAH thermochemolysis was performed for the content of each gut segment.

MATERIALS AND METHODS

Sample Collection and Preparation. Colonies of *C. formosanus* termites, collected in Poplarville, MS, USA, were kept in the laboratory in 5.6 L covered plastic boxes containing blocks of Southern pine wood and moist sand in 90% humidity at 28 ± 1 °C until they were used in experiments. Gut samples were collected by the removal of the body tissue with fine forceps to isolate three whole guts, which were then extended and separated into three parts (foregut, midgut, and hindgut) under a dissection microscope in a sterile condition. On the basis of the larger hindgut volume and small sample size required by Py-GC-MS, three foreguts, three midguts, and two hindguts composed the samples for each gut section. Undigested softwood tissue with a similar particle size of 50 μm was employed as the softwood control sample, whereas the gut segments from termites starved for 3 days and fed on filter paper for another 3 days were employed as the negative control.

Pyrolysis−Methylation Analysis of Gut Contents. Pyrolysis−methylation was performed using 25% (w/w) TMAH in methanol (Sigma-Aldrich, St. Louis, MO, USA) as the derivatizing agent for the characterization of lignin in the biomass, which was converted to its corresponding *N*-and *O*-methyl derivatives by TMAH in the pyrolysis chamber prior to separation and detection by GC-MS. Thermochemolysis reactions of TMAH with lignin in undigested softwood and dissected termite gut segments were carried out rapidly as follows: each sample was placed directly into a quartz sample tube, pulverized with a dissecting needle for better contact of the biomass particles in termite gut with TMAH reagent, and then covered with 0.5 μL of TMAH, respectively. The pyrolysis processes were performed with a

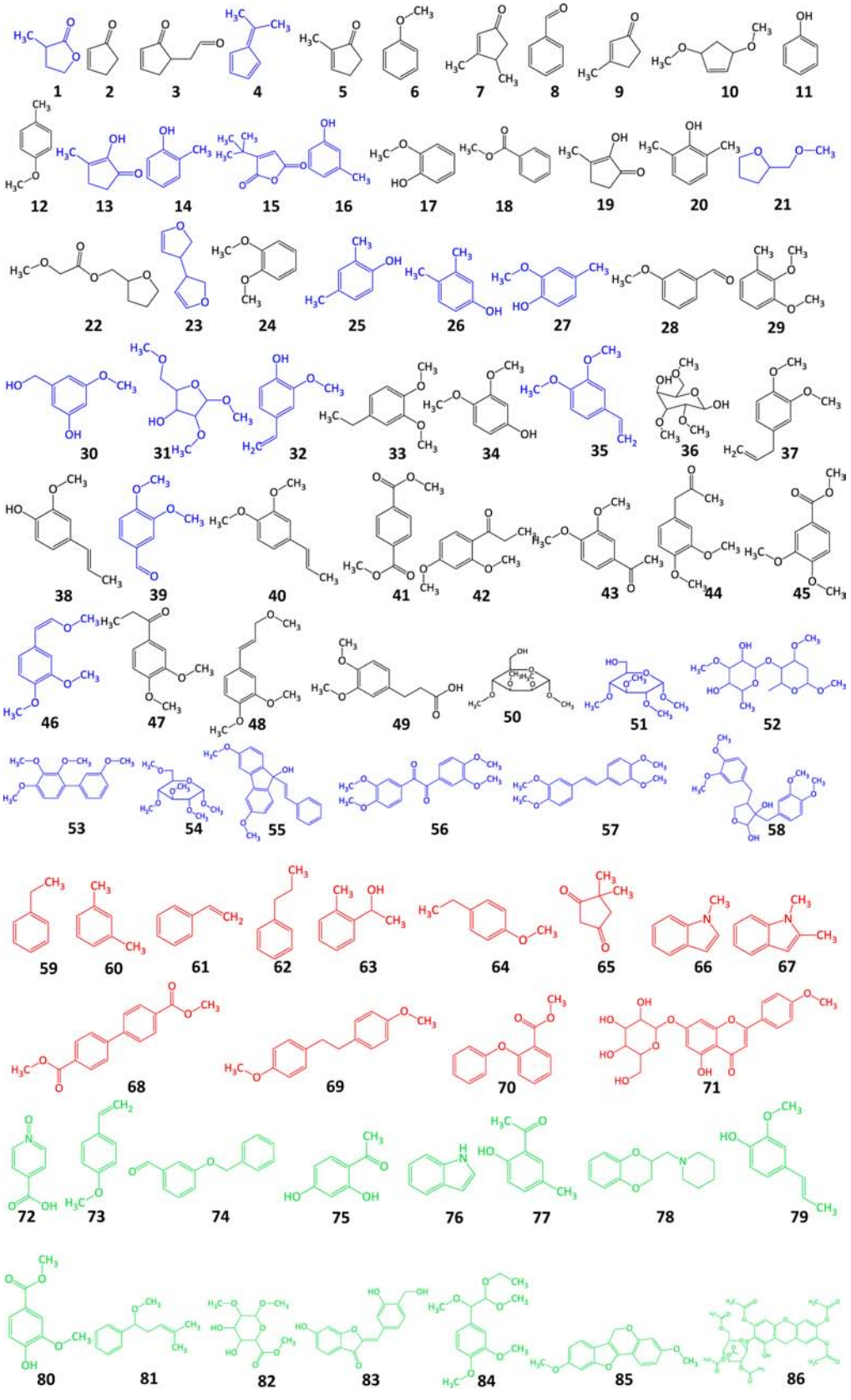

Figure 3. continued

dx.doi.org/10.1021/jf3048548 | J. Agric. Food Chem. 2013, 61, 1299−1308

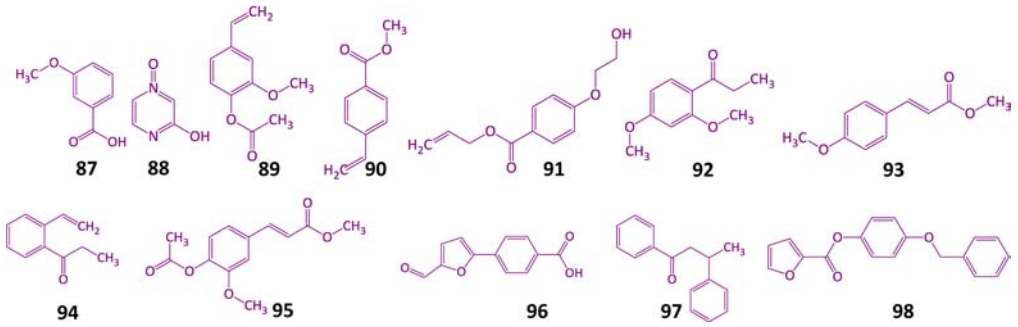

Figure 3. Tentative assignment of all structures of pyrolysates labeled in Figure 2. The methyl groups that may result from methylation by TMAH have been displayed in the structures.

model 5000 pyrolysis autosampler (CDS Analytical, Inc., Oxford, PA, USA) attached to a GC-MS system (Agilent Technologies, Inc., Bellevue, WA, USA). The samples were first preheated at 210 °C for 3 min, then pyrolyzed at a temperature of 510 °C for 1 min, and finally kept in the pyrolysis zone for 56 min. Separation of the volatile products was conducted using a nonpolar HP-5MS capillary column (30 m × 0.25 mm i.d., 0.25 μm, Agilent Technologies, Inc.) with a temperature program from 40 °C (1 min) to 280 °C (15 min) at a rate of 6 °C/min. Helium was used as carrier gas (1 mL/min) in split mode (50:1). Mass identification was performed by interpretation of the EI mass spectra and comparison to NIST MS Search 2.0 electronic libraries. The pyrolysis interface was kept at 210 °C and the GC-MS interface at 280 °C; the GC-MS was programmed to increase the temperature from 40 °C (1 min) to 280 °C (15 min) at a rate of 6 °C/min. The mass spectrometer was operated in EI mode (70 eV) at a source temperature of 230 °C. The eluted pyrolysates were identified by EI mass spectra using the NIST MS Search 2.0 electronic libraries to provide information for softwood metabolites in the termite gut. Each analysis was replicated three times using three different pieces of each sample collected at different times.

RESULTS AND DISCUSSION

The total ion chromatograms (TIC) of Py-TMAH-GC-MS profiles of gut section tissues from cellulose-fed termite are shown in Figure 1. The volatile compounds of indole and fatty acids were generated from gut tissues as labeled in the figure, with minor generation of lignolytic pyrolysates. The TIC derived from the pyrolysis and methylation of the contents from each gut section and the initial softwood control are depicted in Figure 2. Various pyrolysis fragments are generated from the wood biomass by chemical and thermal cleavage at different sites of the phenylpropanoid structure of lignin and produce a typical pyrogram characteristic of lignocellulosic materials. To confirm the structure profile of softwood sample with progressive digestion extent as analyzed by Py-TMAH-GC-MS technique, the major compounds resulting from TMAH derivatization and subsequent thermolysis were compared to that of the control. Thus, the quantitative differences represented by peak height ratios between the relative yields of pyrolysates are considered to be indicative of differences between wood component structures of the original and digested wood (Table 1). The three major pyrolysates of the undigested softwood tissue were all lignolytic compounds, identified as **17**, **57**, and **29**, among which **17** and **29** were considered to be derived from *β*-*O*-4′ substructure,[23,24] whereas pyrolysate **57** is speculated to be generated from pyrolysis of *β*-1′ or *β*-5′ substructure.[25] Apparently, phenolic hydroxyl groups are supposed to be methylated by TMAH, but compound **17** appeared as the most abundant pyrolysate from the undigested softwood. This indicates the block of TMAH from the whole lignin framework by its complex three-dimensional structure and thermally unstable side chain. However, after ingestion by termite and protopepsia in the foregut, the softwood tissue lignin has been modified, as seen in the exhibited pyrolysates **12**, **67**, and **70**. The intensity of peak **12** was due to either *p*-hydroxyphenyl (H) lignin or phenolic demethoxylated guaiacyl (G) lignin, thereby representing a change in the regiochemistry of lignin with increased exposure of the remaining phenolic hydroxyl group to the chemical reagent of TMAH. The newly emerged pyrolysate **67** is speculated to be artificially modified by Py-GC-MS from tryptophan,[26,27] which is a common aromatic amino acid produced de novo by termites,[28,29] or metabolized from lignin.[30] In addition to its involvement in protein synthesis, it acts as a precursor in the synthesis of various N-substituted aromatic secondary metabolites of fungi,[31] which is believed to be the same for termites. Interestingly, tryptophan and its derivatives have been found to be able to stabilize and enhance activity levels of lignin peroxidase and laccase in white rot fungi.[32,33] Thus, tryptophan may also play an important role in wood degradation in termite gut.

Because of this, all of the indolic structures (**66**, **67**, **76**) were assumed to be derived from essential chemicals produced by termite workers for wood digestion, because wood-rot fungus has been reported to produce plant growth regulators, such as indole-3-acetic acid, during the wood digestion process.[34−36] Notably, the dominant pyrolyzed dimer changed from **57** of undigested wood into **70** of the wood particles in the foregut, representing a plausible termite-induced modification of the lignin *β*-1′ or *β*-5′ substructure and side chain, as these substructures are precursors of pyrolysate **57**. With a continued passage of the wood to the midgut, the dominant pyrolysate switched back to **17**. Here the precursor for pyrolysate **17** is believed to be varied from that of the control due to its sharp decrease in the foregut, and the increase of **17** in the midgut may be attributed to lignin conformation change and the presence of more thermally unstable lignin side chains. After completion of digestion in the midgut, subsequent structural modification of lignin was seen to be continued in the hindgut. Besides **12** and **67**, the volatiles originated from wood metabolites pyrolysis changed into **49**, as a result of the obvious carboxylation on aliphatic side chain of lignin. The relative ratios of the other collective pyrolysates of wood tissue before and after termite digestion were also changed due to the functional group change, linkage dissociation, and varied exposure extent of lignin and polysaccharides as shown (Figures 2 and 3).

It is noteworthy that gymnosperm lignin is known to be primarily composed of monomethoxyyphenol units (G).[37] Similarly, the Py-TMAH-GC-MS analysis of control softwood also revealed guaiacyl-derived abundant peaks, which were rich in the methoxy/dimethoxy-substituted benzenoid compounds. These peaks arose from G lignin and retained the major substructural attributes of the β-aryl ether subunits. The reason for this is that TMAH/pyrolysis effectively cleaves the β-aryl ether subunits and renders the released fragments compliant with GC-MS analysis by subsequent methylation.[14,20] In the pyrogram of the undigested control sample, compounds **11**, **13**, **14**, **16**, **19**, **20**, **25**−**27**, **30**−**32**, **34**, **36**, **50**−**52**, **55**, and **58**, which originate from pyrolysis of xylan-, cellulose-, and lignin-derived moieties, were detected mostly as unmethylated derivatives, and many of these peaks disappeared or dramatically decreased in the gut contents. This is due to the fact that the presence of the lignocellulosic matrix prevents chemical access of the derivatizing agent (TMAH) and prohibits facile methylation during the pyrolysis of the untreated softwood tissues. In addition, the selective methylation on the lignin-derived pyrolytic compounds can also be explained through the influence of steric factors influencing the reaction between TMAH and phenolic hydroxyl groups.[11] Decrease of these unmethylated pyrolysates in termite gut revealed wood structure modification during digestion and enhanced exposure of the wood components. Notably, cinnamyl alcohol and aldehyde end groups are also important for the evaluation of the total lignin structure because they can serve as a sensitive index for the structural change and the overall characteristic features of the lignin.[38] Hence, the occurrence of pyrolysates **73**−**75**, **77**, **79**, and **80** in the midgut and **87**, **90**, and **96** in the hindgut, as well as the disappearance of **30**, **32**, **35**, **39**, and **46** in the foregut and **37**, **38**, and **48** in the midgut, in comparison to undigested control indicates lignin modification in the substructural and/or interunit level, as a consequence of the termite lignin-unlocking system, resulting in greater exposure of the lignin end unit to TMAH.

Initiation of Lignin Structural Modification in the Termite Foregut. The termite foregut performs as a valve system (crop-filter chamber) and storage and initial digestion organ. The retention of food in the foregut is from 1 to 2 h, and the emptying in the crop is continuous.[39] In the context of TMAH methylation and thermolysis, the disappearance of pyrolysates **1**, **4**, **13**, **15**, **23**, and **31** and a sharp decrease in the relative intensity of pyrolysates **2**, **5**, and **50**, as well as generation of **65**, in foregut sample shed light on structural change in hemicellulose due to its enhanced exposure with a certain degree of assimilation. Notably, complete disappearance of **51**, **52**, and **54** from the foregut pyrogram also indicated a certain degree of exposed cellulose assimilation. In addition, formation of the new pyrolysate **71** was also evident in the Py-TMAH-GC-MS profile of the foregut content. It is worth mentioning that the substructure of lignin-*O*-carbohydrate cannot be easily conserved during pyrolysis due to the low thermal stability of ether bonds between lignin and carbohydrate. This helps to explain the nonexistence of compounds **71** and **86** in undigested softwood control. Thus, detection of **71** in the foregut suggests there is modification of lignin−carbohydrate association resulting in the release of volatile and thermally stabilized fragmented pyrolyzed product of lignin-*O*-carbohydrate ether-linked origin. Relative intensity change of compounds **6**, **11**, **12**, **29**, and **33** and disappearance of **14**, **16**, **25**, **26**, **27**, **30**, **32**, **35**, **39**, **46** in the foregut sample provided evidence of lignin side-chain modification, indicating lignin conformation change thereafter, which could also be supported by the disappearance of pyrolysates **55**, **56**, and **58**. The disappearance of compound **53** in the pyrogram of this gut section represents plausible cleavage of C−C/C−O within the 5-5′ substructure, accompanied by the condensation afterward. Especially, side-chain carboxylation and phenolic dehydroxylation are indicated to be initiated in the foregut due to the relatively increased intensity of **49** and the occurrence of **62** and **63**, respectively. Kuroda et al.[25] have reported structure **57** could originate from lignolytic β-5′ substructure. Thus, the disappearance of **57** during foregut pyrolysis indicates termite-induced modification on the β-5′ substructure, which led to the subsequent change of the related pyrolysate. The abundant presence of pyrolysate **70** in the foregut sheds light on the modification adjoining the 4-*O*-5′ substructure of lignin, resulting in thermally stabilized 4-*O*-5′ linkages. The phenolic dehydroxylation and side-chain esterification/etherification are further supported by the occurrence of pyrolysates **68** and **69**, which indicates modification of the β-1′ substructure initiated in the foregut.[40]

Selective Lignin Structural Modification Mainly Happening in the Midgut. The retention time for food passage through the midgut is similar to that of the foregut. Also, it has been demonstrated that there is no reflux of food from the hindgut to the midgut.[39] The midgut of wood-feeding lower termite is comparatively longer than that of the higher termite,[41] which is speculated to result from a varied diet and because wood digestion by lower termites requires a more intensive lignin pretreatment process. In general, a variety of new pyrolysates generated in much abundance from the wood metabolites in the midgut indicated further lignin disruption. The disappearance of pyrolysate **71** and the occurrence of **86** derived from lignin-*O*-carbohydrate association represented a continued modification on lignin−carbohydrate linkage in the termite midgut and thus the generation of more volatile and thermally stable lignin-*O*-carbohydrate ether-linked pyrolysates. In addition, compound **72** was also evident in the Py (TMAH)-GC-MS profile of the midgut sample. It is probably derived thermally from the lignin decomposition intermediate of termites, such as 4-methoxyphenol,[42] and also a further indication of phenolic carboxylation. In particular, phenolic dehydroxylation and side-chain oxidation were also documented by the occurrence of **74** and **81**, as well as the phenolic demethoxylation and carbonylation, which were indicated by **75** and **77**, respectively. Obviously, the relative intensity of pyrolysate **49** was significantly enhanced and indicative of continued lignin side-chain carboxylation. The continued lignin side chain modification resulted in change of the midgut pyrogram, in which both the occurrence of compounds **73** and **83** and the disappearance of various compounds (**24**, **28**, **29**, **33**, **34**, **37**, **40**, **44**, and **48**) were observed. Importantly, the occurrence of derived lignolytic compound **84** in the pyrogram of the midgut-metabolized wood sample represents the regiochemistry of the β-*O*-4′ (β-aryl ether) linked phenyl glycerol containing subunits in lignin, as reflected from the selective labeling studies previously presented by Filley et al.[14] Some other changes of the peak elution of termite midgut include the disappearance of dimer **69** and the occurrence of **83** and indole **76**, which should be thermally derived from modified lignin β-1′ and β-5′ substructures, respectively.[30,40] A newly emerged pyrolysate, **74**, was considered to be derived from the modified α-*O*-4′ substructure of lignin. All of the

selective lignin structural modification occurred in the termite midgut as summarized above, which as a result would lead to the conformation change of lignin matrix, represented by the disappearance of compounds **18**, **20**, and **62**, and the appearance of **79** and **80**. Besides the lignin disruption, assimilation of hemicelluloses and cellulose was also detected in the midgut, indicated by the disappearance of pyrolysates **7**, **9**, **10**, **36**, and **50** and the appearance of **82**. Additionally, the formation of product **85** induced by the termite digestive system suggested a possible condensed structure formation in the resulting lignin-derived polymer in the midgut-contained softwood tissues while retaining the abundant *β*-*O*-4′ interunit linkage and most of its original aromatic residues, which were probably interconnected by additional interunit linkages.

Continued Lignin Structural Modification in Hindgut. Food passage is significantly slower in the hindgut segment, with a retention time of 14−20 h.[39] Consequently, this gut segment is well-studied and is believed to be the location of cellulose hydrolysis.[43] Therefore, it is logical to be considered as a microbial niche for degradation of lignin oligmers generated from the midgut, further alleviating the inhibitory effect on cellulose hydrolysis.[44] As shown in the pyrogram of the hindgut contents (Figure 2), the pyrolysate profile of the hindgut metabolites was qualitatively similar to that of the midgut except for the presence and disappearance of a few pyrolysates. The continued disappearances of xylan-derived pyrolysates **3** and **5** were considered to be indicative of further hemicelluloses assimilation in the hindgut. The ether linked lignin−cellulose structure could not be observed in the pyrogram from the digested wood in the hindgut, as a result of further modification on lignin−cellulose association in the hindgut. The new pyrolysis occurrence of C−C-linked (pyrolysate **96**) and ester-linked (pyrolysate **98**) aromatic−furfural molecules in the hindgut also indicated further modification of the lignin−hemicellulose association, which may result from polyssacharide degradation and stabilized aromatic−furfural complex. Likewise, further lignin side-chain oxidation and modification were also evident in the hindgut by the disappearance of pyrolysate **84**, the occurrence of **91**−**93** and **95**, and the significant decrease of compound **17**. Compound **91** is considered to be derived from lignin structure with an oxidized and esterified/etherified side chain, and **92** was generated from aliphatic carbonylated lignolytic structure. The origin of **89**, **93**, and **95** is attributed to lignin phenolic functional group change and side-chain esterification. Obviously, compounds **70** and **77** with abundant intensity in the fore- and midgut disappeared in the hindgut; the reason for this is speculated to be the further modification of lignin side-chain or phenolic functional group(s). In addition, the termite-induced modification of the lignin phenolic ring was clearly demonstrated by the occurrence of compounds **87**−**91** and **93**−**97** from this gut segment. To be specific, the unique structure of compound **88** was considered to be of termite origin, which would have an impact on the final lignin pretreatment for subsequent cellulose hydrolysis. Compounds **87** and **96** indicated phenolic carboxylation and **90**, **91**, **94**, and **98** suggested phenolic dehydroxylation, demethoxylation, and esterification. The decreased intensity of derived compound **17** in the pyrogram of the hindgut sample also represents the regiochemistry change of G lignin, resulting in greater exposure of the phenolic hydroxyl group to the chemical reagent of TMAH. Similarly, the disappearance of compounds **60**, **79**, and **80** in the pyrogram of the hindgut represented greater exposure of G-lignin, which is speculated to be attributed to the lignin ether linkage cleavage and/or phenolic functional group change, which induces a conformational change in the lignin network. In fact, there have been studies demonstrating the isolation of microorganisms within the termite hindgut that are responsible for aromatic lignin model compound degradation.[45,46] It has also been reported that the oligomeric lignin is degraded in the termite hindgut.[47] On this basis, together with our previous study,[5,44,48] it is proposed that lignin structural modification in the hindgut results from a combined effect of hindgut symbiotic microbes and continued action of wood-adsorbed lignin-modifying factor(s) from the midgut.

Overall, Py-GC-MS in the presence of TMAH showed a selective cleavage of *β*-*O*-4′ linkages and subsequent methylation of all ring hydroxyls that were represented by the generation of abundant new pyrolyzates. This signifies that the pyrolysis−methylation analysis helped to extract more information for the absolute structural change of lignin compared to the ambiguous pyrolysis cleavage by normal flash Py-GC-MS analysis.[49] Thus, Py(TMAH)-GC-MS analysis provides support for the modification on specific lignin functional groups and linkages that are supposed to happen stepwise along the whole of the termite gut, to help with the unlocking of polyssaccharides. The calculated ratio of lignolytic pyrolysates for control and the three gut segments is 1/1.17/1.12/1.10. The increase of pyrolyzed lignolytic volatiles from undigested softwood control to foregut sample is considered to be attributed to the lignin conformation change caused by structural modification during chewing and foregut metabolism. The slight decrease of lignolytic pyrolysates from the foregut to the midgut and hindgut sheds light on the condensation of structure-modified lignin.[6,7] Furthermore, the ratios of lignin H units and methylated ones for the four samples are 1/0.47, 1/1.35, 1/0.77, and 1/1.60, respectively, and those of G units and methylated forms are 1/1.88, 1/6.22, 1/0.77, and 1/7.00, respectively. The methylated forms of both H and G lignin units increased in the foregut, decreased in the midgut, and increased again in the hindgut. It is surmised that this is attributed to lignin conformation change resulting from the initial structural modification in foregut. With continued modification, the modified lignin was condensed in the midgut and thus protected from TMAH. When the gut fluid passed through the hindgut, more lignin was exposed to TMAH because of the polysaccharide assimilation there. Notably, the foregut was found to be the site for the initiation of modification on lignin−polyssaccharide association and substructure of 5-5′, *β*-5′, *β*-1′, side-chain oxidation and carboxylation, and phenolic dehydroxylation; all of these reactions continued in the midgut, and more modifications such as phenolic carboxylation, demethoxylation, and carbonylation also happened in this segment. With continued food passage into the hindgut, the lignin side-chain and phenolic esterifications were proved to be the main reaction there. Therefore, continued from the feces analysis, advanced TMAH thermochemolysis of the content of each gut segment helped elucidate the stepwise unlocking process in each gut section, and the leading role of midgut in lignin structure modification suggests it as the main place for the lignin unlocking process for polysaccharide release before hydrolysis in the hindgut, which further confirms our previous speculation.[5]

This study updates our previous studies of the mechanism of lignin structural modification in termite.[5−7] Previously, the digestive system of termite acted as a black box. All of the

characterizations of termite feces revealed only some reactions occurring inside the black box, but were not conclusive due to the difficulty in collection of gut contents.[6,7,50] Instead, monitoring the lignin structure change in each gut segment helped us explore the black box with the aid of Py (TMAH)-GC-MS. Speculations of selective lignin structural modification in termite gut, such as lignin−polyssaccharides dissociation, lignin side-chain oxidation, and phenolic dehydroxylation and demethoxylation, were confirmed in this study[5−7] and were determined to be initiated in the foregut and midgut, respectively. Moreover, some other structural modifications of lignin were identified, such as lignin side-chain carboxylation starting from the foregut, phenolic carboxylation and carbonylation in the midgut, and lignin esterification in the hindgut.

All of these results suggest that the plant cell wall deconstruction process of this termite species consists of multiple stepwise unlocking reactions. Such an unlocking process mainly affected the lignin matrix and lignin−polysaccharide association, which makes this process unique in the approach to biomass pretreatment. This study reveals the advantages of wood-feeding termites over wood-rot fungi and other lignocellulosic-degrading microbes, in that it works as a highly effective continuous and well-integrated system for stepwise deconstruction of the lignin−hemicellulose matrix. This effective wood degrader provides us with a new scientific base for stepwise modification on selected functional groups and linkages, which might contribute to the current understanding of specific unlocking modifications on lignin structure by the lower termites for efficient cellulose utilization, as well as potentially promoting the development and customization of a new pretreatment technology for effective disintegration of the plant cell wall structure to produce bioenergy-derived value-added coproducts and fuels. Notably, a lignin-modifying system mimicking the termite will be advanced in rate, selectivity, and neutral working conditions. The process does not largely affect the lignin backbone and thus consumes less energy and produces negligible lignin-derived inhibitors for subsequent cellulose hydrolysis and sugar fermentation. Meanwhile, the residual lignin backbone may be promising for application to other purposes such as value-added lignolytic coproducts to reduce the pretreatment cost.

AUTHOR INFORMATION

Corresponding Author

*Phone: +1 (509) 335-3743. Fax: +1 (509) 335-2722. E-mail: chens@wsu.edu.

Funding

This work was financially supported by the National Science Foundation (NSF Grant 1231085) and by the Agricultural Research Center of Washington State University (WSU).

Notes

The authors declare no competing financial interest.

ABBREVIATIONS USED

TMAH, tetramethylammonium hydroxide; Py-GC/MS, pyrolysis−gas chromatography−mass spectrometry; TIC, total ion chromatograms; H lignin/unit, *p*-hydroxyphenyl lignin/unit; G lignin/unit, guaiacyl lignin/unit

REFERENCES

(1) National Research Council, Committee on economic and environmental impacts of increasing biofuels production. National Academy of Sciences, 2011.

(2) Hisano, H.; Nandakumar, R.; Wang, Z. Genetic modification of lignin biosynthesis for improved biofuel production. *In Vitro Cell. Dev. Biol: Plant* **2009**, *45*, 306−313.

(3) Weng, J.; Li, X.; Bonawitz, N. D.; Chapple, C. Emerging strategies of lignin engineering and degradation for cellulosic biofuel production. *Curr. Opin. Biotechnol.* **2008**, *19*, 166−172.

(4) Chandra, R. P.; Bura, R.; Mabee, W. E.; Berlin, A.; Pan, X.; Saddler, J. N. Substrate pretreatment: the key to effective enzymatic hydrolysis of lignocellulosics? *Biofuels* **2007**, *108*, 67−93.

(5) Ke, J.; Sun, J.; Nguyen, H. D.; Singh, D.; Lee, K. C.; Beyenal, H.; Chen, S. In-situ oxygen profiling and lignin modification in guts of wood-feeding termites. *Insect Sci.* **2010**, *17*, 277−299.

(6) Ke, J.; Singh, D.; Chen, S.; Yang, X. Thermal characterization of softwood lignin modification by termite *Coptotermes formosanus* (Shiraki). *Biomass Bioenerg.* **2011**, *35*, 3617−3626.

(7) Ke, J.; Laskar, D. D.; Singh, D.; Chen, S. In-situ lignocellulosic unlocking mechanism in termite for cellulose hydrolysis: critical lignin modification. *Biotechnol. Biofuels* **2011**, *4*, 17−23.

(8) Pan, X. Role of functional groups in lignin inhibition of enzymatic hydrolysis of cellulose to glucose. *J. Biobased Mater. Bioenergy* **2008**, *2*, 25−32.

(9) Nakagame, S.; Chandra, R. P.; Kadla, J. F.; Saddler, J. N. Enhancing the enzymatic hydrolysis of lignocellulosic biomass by increasing the carboxylic acid content of the associated lignin. *Biotechnol. Bioeng.* **2011**, *108*, 538−548.

(10) Challinor, J. M. A pyrolysis-derivatisation-gas chromatography technique for the structural elucidation of some synthetic polymers. *J. Anal. Appl. Pyrolysis* **1989**, *16*, 323−333.

(11) Challinor, J. M. Characterisation of wood by pyrolysis derivatisation-gas chromatography/mass spectrometry. *J. Anal. Appl. Pyrolysis* **1995**, *35*, 93−107.

(12) Challinor, J. M. The development and applications of thermally assisted hydrolysis and methylation reactions. *J. Anal. Appl. Pyrolysis* **2001**, *61*, 3−34.

(13) Clifford, D. J.; Carson, D. M.; McKinney, D. E.; Bortiatynski, J. M.; Hatcher, P. G. A new rapid technique for the characterization of lignin in vascular plants: thermochemolysis with tetramethylammonium hydroxide (TMAH). *Org. Geochem.* **1995**, *23*, 169−175.

(14) Filley, T. R.; Minard, R. D.; Hatcher, P. G. Tetramethylammonium hydroxide (TMAH) thermochemolysis: proposed mechanisms based upon the application of ^{13}C-labeled TMAH to a synthetic model lignin dimer. *Org. Geochem.* **1999**, *30*, 607−621.

(15) Schulten, H. R.; Gleixner, G. Analytical pyrolysis of humic substances and dissolved organic matter in aquatic systems: structure and origin. *Water Res.* **1999**, *33*, 2489−2498.

(16) Geffroy-Rodier, C.; Grasset, L.; Sternberg, R.; Buch, A.; Amblès, A. Thermochemolysis in search for organics in extraterrestrial environments. *J. Anal. Appl. Pyrolysis* **2009**, *85*, 454−459.

(17) Fu, S. Y.; Lucia, L. A. TMAH-pyrolysis-gas chromatographymass spectrometry analysis of residual lignin changes in softwood kraft pulp during oxygen delignification. *Can. J. Chem.* **2004**, *82*, 1197−1202.

(18) Kuroda, K. I.; Nakagawa-izumi, A. Tetramethylammonium hydroxide (TMAH) thermochemolysis of guaiacyl-syringyl and guaiacyl dehydrogenation polymers. *Org. Geochem.* **2005**, *36*, 53−61.

(19) González-Vila, F. J.; Almendros, G.; Del Río, J. C.; Martin, F.; Gutiérrez, A.; Romero, J. Ease of delignification assessment of wood from different Eucalyptus species by pyrolysis (TMAH)-GC/MS and CP/MAS ^{13}C-NMR spectrometry. *J. Anal. Appl. Pyrolysis* **1999**, *49*, 295−305.

(20) Kuroda, K.; Nishimura, N.; Izumi, A.; Dimmel, D. R. Pyrolysis of lignin in the presence of tetramethylammonium hydroxide: a convenient method for S/G ratio determination. *J. Agric. Food Chem.* **2002**, *50*, 1022−1027.

(21) Sun, J. Z.; Zhou, X. G. Utilization of lignocellulose-feeding insects for viable biofuels: an emerging and promising area of

entomological science. In *Recent Advances in Entomological Research*, 1st ed.; Liu, T. X., Kang, L., Eds.; Higher Education Press: Beijing, China, 2010; pp 251−291.
(22) Ke, J.; Laskar, D. D.; Gao, D.; Chen, S. Advanced biorefinery in lower termite − effect of combined pretreatment during the chewing process. *Biotechnol. Biofuels* **2012**, *5*, 11−24.
(23) Kuroda, K.; Nakagawa-Izumi, A. Tetramethylammonium hydroxide (TMAH) thermochemolysis of lignin: behavior of 4-*O*-etherified cinnamyl alcohols and aldehydes. *J. Agric. Food Chem.* **2005**, *53*, 8859−8865.
(24) Chu, S.; Subrahmanyam, A. V.; Huber, G. W. The pyrolysis chemistry of a β-*O*-4 type oligomeric lignin model compound. *Green Chem.* **2013**, *15*, 125−136.
(25) Kuroda, K.; Nakagawa-Izumi, A.; Dimmel, D. R. Pyrolysis of lignin in the presence of tetramethylammonium hydroxide (TMAH): products stemming from β-5 substructures. *J. Agric. Food Chem.* **2002**, *50*, 3396−3400.
(26) Gallois, N.; Templier, J.; Derenne, S. Pyrolysis−gas chromatography−mass spectrometry of the 20 protein amino acids in the presence of TMAH. *J. Anal. Appl. Pyrolysis* **2007**, *80*, 216−230.
(27) Stankiewicz, B. A.; Hutchins, J. C.; Thomson, R.; Briggs, D. E. G.; Evershed, R. P. Assessment of bog-body tissue preservation by pyrolysis-gas chromatography/mass spectrometry. *Rapid Commun. Mass Spectrom.* **1997**, *11*, 1884−1890.
(28) Shigenobu, S.; Watanabe, H.; Hattori, M.; Sakaki, Y.; Ishikawa, H. Genome sequence of the endocellular bacterial symbiont of aphids *Buchnera* sp. APS. *Nature* **2000**, *407*, 81−86.
(29) Hongoh, Y.; Sharma, V. K.; Prakash, T.; Noda, S.; Taylor, T. D.; Kudo, T.; Sakaki, Y.; Toyoda, A.; Hattori, M.; Ohkuma, M. Complete genome of the uncultured termite group 1 bacteria in a single host protist cell. *Proc. Natl. Acad. Sci U.S.A.* **2007**, *105*, 5555−5560.
(30) Fernandes, D. M.; Hechenleitner, A. A. W.; Job, A. E.; Radovanocic, E.; Pineda, E. A. G. Thermal and photochemical stability of poly(vinyl alcohol)/modified lignin blends. *Polym. Degrad. Stab.* **2006**, *91*, 1192−1201.
(31) Turner, W. B.; Aldridge, D. C. Secondary metabolites derived from amino-acids. In *Fungal Metabolites*, 1st ed.; Turner, W. B., Aldridge, D. C., Eds.; Academic Press: London, UK, 1983; Vol. *I*, pp385−457.
(32) Collins, P. J.; Field, J. A.; Teunissen, P.; Dobson, A. D. Stabilization of lignin peroxidases in white rot fungi by tryptophan. *Appl. Environ. Microbiol.* **1997**, *63*, 2543−2548.
(33) Eggert, C.; Temp, U.; Dean, J. F. D.; Eriksson, K. E. L. A fungal metabolite mediates degradation of non-phenolic lignin structures and synthetic lignin by laccase. *FEBS Lett.* **1996**, *391*, 144−148.
(34) Yürekli, F.; Geckil, H.; Topcuoglu, F. The synthesis of indole-3-acetic acid by the industrially important white-rot fungus *Lentinus sajor-caju* under different culture conditions. *Mycol. Res.* **2003**, *107*, 305−309.
(35) Tuomi, T.; Ilvesoksa, J.; Laakso, S.; Rosenqvist, H. Interaction of abscisic acid and indole-3-acetic acid producing fungi with *Salix* leaves. *J. Plant Growth Regul.* **1993**, *12*, 149−156.
(36) Yürekli, F.; Yesilada, O.; Yürekli, M.; Topcuoglu, S. F. Plant growth hormone production from olive oil mill and alcohol factory wastewaters by white rot fungi. *World J. Microbiol. Biotechnol.* **1999**, *15*, 503−505.
(37) Yokoi, H.; Nakase, T.; Ishida, Y.; Ohtani, H.; Tsuge, S.; Sonoda, T.; Ona, T. Discriminative analysis of *Eucalyptus camaldulensis* grown from seeds of various origins based on lignin components measured by pyrolysis−gas chromatography. *J. Anal. Appl. Pyrolysis* **2001**, *57*, 145−152.
(38) Lai, Y. Z.; Sarkanen, K. V. Isolation and structural studies. In *Lignins Occurrence, Formation, Structure and Reactions*, 1st ed.; Sarkanen, K. V., Ludwig, C. H., Eds.; Wiley: New York, 1971; pp165−240.
(39) Kovoor, J. Etude radiographique du transit intestinal chez un Termite supérieur. *Cell. Mol. Life Sci.* **1967**, *23*, 820−821.
(40) Kuroda, K.; Ashitani, T.; Fujita, K.; Hattori, T. Thermal behavior of β-1 subunits in lignin: pyrolysis of 1,2-diarylpropane-1,3-diol-type lignin model compounds. *J. Agric. Food Chem.* **2007**, *55*, 2770−2778.
(41) Noirot, C. H.; Noirot-Timothee, C. The digestive system. In *Biology of Termites*; Krishna, K., Weesner, F. M., Eds.; Academic Press: New York, 1969; Vol. *1*, pp 49−88.
(42) Bremner, J. M. Organic nitrogen in soils. In *Soil Nitrogen*; Bartholomew, W. V., Clark, F. E., Eds.; American Society of Agronomy Monograph: Madison, WI, 1965; pp93−149.
(43) Warnecke, F.; Luginbühl, P.; Ivanova, N.; Ghassemian, M.; Richardson, T. H.; Stege, J. T.; Cayouette, M.; McHardy, A. C.; Djordjevic, G.; Aboushadi, N.; Sorek, R.; Tringe, S. G.; Podar, M.; Martin, H. G.; Kunin, V.; Dalevi, D.; Madejska, J.; Kirton, E.; Platt, D.; Szeto, E.; Salamov, A.; Barry, K.; Mikhailova, N.; Kyrpides, N. C.; Matson, E. G.; Ottesen, E. A.; Zhang, X.; Hernández, M.; Murillo, C.; Acosta, L. G.; Rigoutsos, I.; Tamayo, G.; Green, B. D.; Chang, C.; Rubin, E. M.; Mathur, E. J.; Robertson, D. E.; Hugenholtz, P.; Leadbetter, J. R. Metagenomic and functional analysis of hindgut microbiota of a wood-feeding higher termite. *Nature* **2007**, *450*, 560−565.
(44) Ke, J.; Singh, D.; Chen, S. Aromatic compound degradation by the wood-feeding termite *Coptotermes formosanus* (Shiraki). *Int. Biodeter. Biodegr.* **2011**, *65*, 744−756.
(45) Harazono, K.; Yamashita, N.; Shinzato, N.; Watanabe, Y.; Fukatsu, T.; Kurane, R. Isolation and characterization of aromatics-degrading microorganisms from the gut of the lower termite *Coptotermes formosanus*. *Biosci., Biotechnol., Biochem.* **2003**, *67*, 889−892.
(46) Kuhnigk, T.; König, H. Degradation of dimeric lignin model compounds by aerobic bacteria isolated from the hindgut of xylophagous termites. *J. Basic Microbiol.* **1997**, *37*, 205−211.
(47) Cookson, L. J. The site and mechanism of ^{14}C-lignin degradation by *Nasutitermes exitiosus*. *J. Insect Physiol.* **1988**, *34*, 409−414.
(48) Ke, J.; Singh, D.; Chen, S. Metabolism of polycyclic aromatic hydrocarbons by the wood-feeding termite *Coptotermes formosanus* (Shiraki). *J. Agric. Food Chem.* **2012**, *60*, 1788−1797.
(49) Filley, T. R. *Wood Deterioration and Preservation: Advances in Our Changing World*; ACS Symposium Series 845; Goodwell, B., Nicholas, D. D., Schultz, T. P., Eds.; American Chemical Society: Washington, DC, 2003; pp119−139.
(50) Geib, S. M.; Filley, T. R.; Hatcher, P. G.; Hoover, K.; Carlson, J. E.; Jimenez-Gasco, M. M.; Nakagawa-Izumi, A.; Sleighter, R. L.; Tien, M. Lignin degradation in wood-feeding insects. *Proc. Natl. Acad. Sci U.S.A.* **2008**, *105*, 12932−12937.